

Spectral diffusion from stimulated spin echoes of phosphorescent F_2^{2+} centers in MgO

R. Vreeker, M. W. L. Bovy, and M. Glasbeek

Laboratory for Physical Chemistry, University of Amsterdam, Nieuwe Achtergracht 127, 1018-W5 Amsterdam, The Netherlands

(Received 14 July 1983)

Nonstationary spectral diffusion is observed for F_2^{2+} centers, in MgO, in the photoexcited ${}^3B_{1u}$ state by means of optically detected stimulated-echo-decay experiments. It is discussed that two different spectral diffusion processes can be probed for the photoexcited F_2^{2+} -center triplet spins. In addition to the recently reported diffusion due to time-dependent AB -spin interactions, we report here a slower spectral diffusion process that is attributed to a migration of optical ${}^3B_{1u} \rightarrow {}^1A_g$ transition energy or electron tunneling processes in the MgO host.

I. INTRODUCTION

Phase and energy relaxation of optically active ions or defects in solids are studied to better understand the mechanisms for radiative and radiationless transitions, energy transfer, or photoinduced charge transport.¹ To eliminate the effects of inhomogeneous broadening, which in the condensed phase usually far exceeds the homogeneous linewidth, powerful pulse techniques have been developed which allow us to examine directly in the time-domain population relaxation (T_1 type) and pure or phase relaxation (T_2 type). In the particular case of photoexcited triplet states, considerable work has been done using techniques for the optical detection of spin-coherent transients; for excellent reviews regarding recent studies on organic molecular crystals and systems of biophysical interest see Refs. 2–4.

In recent years, triplet-spin coherence has also been observed for photoexcited color centers in ionic solids.^{5–7} In the experiments, a coherent superposition state is created by means of a high-power microwave pulse resonant with one of the possible triplet-spin transitions; coherence persists during the time the pulse-induced molecular magnetic moments oscillate in phase and are well defined. Much attention was given to the problem of irreversible relaxation of the coherent state, or equivalently, the mechanism responsible for homogeneous broadening.

It was shown,^{6,7} that the probed spins (called A spins) exhibit dephasing because of magnetic dipolar contact with fluctuating neighboring spins (referred to as B spins). Under the influence of the B spins, A spins experience local-field fluctuations which spread out the A -spin frequencies (spectral diffusion). Concomitant with this spectral diffusion, the A spins undergo in phase space random-phase excursions which effect phase relaxation.

As detailed later, it is useful to distinguish between stationary and nonstationary spectral diffusion. Illustrative manifestations of the latter have been measured in fluorescence or phosphorescence line-narrowing experiments^{8,9} and in stimulated–spin-echo–decay (SED) experiments.¹⁰ Typically, in these experiments one is able to directly probe the redistribution with time of optical or microwave excitations that results from energy transfer. On the other hand, when steady-state conditions prevail and the spec-

tral distribution function is time independent, the temporal effects in the frequency domain are said to be stationary.

In this paper we report on a nonstationary spectral-diffusion process involving triplet-spin excitations of photoexcited color centers. We focus on stimulated–spin-echo decays as measured for F_2^{2+} centers in MgO in the photoexcited ${}^3B_{1u}$ state.^{11,12} In discussing the SED results, a comparison with our previous spin-dephasing data⁷ is included. We will argue that, whereas the dephasing occurs due to spin-spin interactions in the stationary diffusion regime, the spectral changes responsible for the SED originate in a different (nonstationary) spectral-diffusion process. Most probably, for this (slower) process transfer of the optical excitation energy of the ${}^3B_{1u}$ state or electron tunneling is involved.

The phase-relaxation dynamics for the F_2^{2+} (MgO) system in the ${}^3B_{1u}$ state was previously analyzed using a memory-function formalism.⁷ To discuss the relationship between the SED results of this work and the Hahn-echo results obtained before, it was thought useful to briefly reproduce the main features of the memory-function approach (Sec. II). In this section the conditions for measuring a decay of the stimulated-echo signal are indicated also. In Sec. III, the experimental part, we have included for those not familiar with double-resonance spin-coherence techniques, a brief overview of the experimental methods used in this work. The results and their discussion are presented in Secs. IV and V.

II. STATIONARY AND NONSTATIONARY SPECTRAL DIFFUSION

Measurements of zero-field spin transitions involving alkaline-earth–oxide F_2^{2+} centers in the ${}^3B_{1u}$ state have revealed linewidths of about 10 MHz full width at half maximum.¹¹ Spin-echo–decay measurements under similar experimental circumstances, typically yield decay times varying between 150 and 200 μ s at liquid-helium temperatures. Clearly, the magnetic resonance transitions are inhomogeneously broadened. Most likely, the inhomogeneous spread in the resonance frequencies is caused by the interaction of the photoexcited triplet spins with randomly distributed static strain fields in the host crys-

tal. In zero field the triplet-spin angular momentum is quenched.⁶ This quenching is (partially) lifted upon the application of either a static magnetic field or a resonant microwave radiation field. It is due to this unquenching that the $S=1$ spins become affected by the randomly fluctuating B spins.

In the echo experiments of interest here, the irreversible decay of a (pseudo)magnetization component S_1 is followed. S_1 comprises the magnetic-moment contributions of a collection of inhomogeneously dispersed isochromats. Actually, since in the echo pulse cycle inhomogeneous broadening effects are eliminated, the fate of each individual S_{1i} is traced (S_{1i} denotes the magnetization due to the i th isochromat). In general, S_{1i} is due to A spins with identical microwave resonance frequencies Ω_i , i.e., these A spins are subject to similar secular strain-induced shifts. At the same time, these A spins may still be different in that the spatial arrangement of the surrounding B spins may show some variation. In the following, it is advantageous to first consider the time evolution of the echo amplitude due to a subset (k) of identical triplet (A) spins for which the resonance frequency Ω_i and the surrounding B -spin configuration are similar. Then, it can be derived⁶ that

$$\frac{dS_{1ik}^*(t)}{dt} = -s(t) \sum_j \int_0^t dt' s(t') K_{ij}(t-t') S_{1jk}^*(t'). \quad (1)$$

In Eq. (1), $S_{1ik}^*(t)$ is the transition moment characteristic of the subset k in isochromat i , viewed in a frame rotating at frequency Ω_i ; $s(t)$ is a step function reflecting the changes induced by the microwave pulses in the SED experiment, i.e., $s(t)=1$ for $0 < t < \tau$, $s(t)=0$ for $\tau < t < (\tau+T)$, and $s(t)=-1$ for $t > (\tau+T)$, where τ and T specify the conditions of the SED experiment as explained in Sec. III. $K_{ij}(t-t')$ represents the (i,j) th element of the triplet-spin memory tensor, where it is noted that the diagonal elements, according to the second fluctuation-dissipation theorem,³ are related to the auto-correlation function of the B spins.

Obviously, the dynamical details of the spectral-diffusion process are contained in the time behavior of the memory-function tensor \vec{K} . For example, the off-diagonal elements, K_{ij} for $i \neq j$, are characteristic of cross correlation between different isochromats, and thus are the cause for nonstationary diffusional effects in the time domain. On the other hand, when all nondiagonal couplings (including those among the A and the B spins) are omitted, one obtains the time behavior of the A -spin magnetization in the stationary diffusion regime. As a matter of fact, in this stationary limit, and taking $T=0$, exact solutions of Eq. (1) could be obtained assuming a monoexponentially decaying memory function.⁷ We remark that the stationary regime will prevail in two limiting cases.

In the first, the so-called slow-exchange limit, the characteristic B -spin relaxation rate R is small compared to the AB interaction strength Δ . Here Δ denotes the square root of the second moment of the A -spin resonance due to the AB -dipolar interaction. For the slow-motion limit it was calculated that a line splitting in the A -spin

spectrum results, the splitting being characteristic of Δ .⁷ Moreover, the split lines were shown to be broadened due to the relatively slow B -spin reorientations. Thus, in the limit where $\Delta/R \gg 1$, exchange effects are negligible and the dephasing rate (as, e.g., measured in a Hahn-echo experiment) of the A -spin subset k will be of the order of R . This approach was taken when discussing the spin dephasing of photoexcited F_2^{2+} centers in CaO, although to obtain the expression for the echo decay observable in this case an additional averaging over all possible B -spin configurations, $\langle S_{1ik}^*(2\tau) \rangle_k$, had to be performed.⁶ Now when we allow for dynamical exchange between the inhomogeneously dispersed A -spin resonances due to B -spin flippings (but retain $\Delta/R > 1$), the nonstationary regime applies. The additional phenomena that may arise when performing a Hahn-echo experiment in this regime, were extensively discussed in our previous paper.⁷ Independent evidence for a nonstationary diffusion process is obtained in a stimulated-echo (SE) experiment. When the SE amplitude decays on a time scale much shorter than that corresponding to the population relaxation of the resonantly coupled spin levels, nonstationary spectral diffusion is present. To describe the SED quantitatively, complete knowledge of the A -spin memory-function tensor $\vec{K}(t)$ is required. Most often, such detailed information is lacking, although recently a spectral-diffusion model was presented which basically includes the effects that derive from the off-diagonal elements of $\vec{K}(t)$.¹⁴ For all practical purposes, the phenomenological approaches developed a long time ago^{15,16} are most useful. In these approaches expressions were derived for the coherence decay when assuming a functional form for the diffusion kernel in a number of cases; in the SED experiment the Fourier transform of this diffusion kernel is measured.

Finally, we briefly consider the other limiting situation for which the spectral distribution turns out to be stationary. As already discussed in detail elsewhere,⁷ for $\Delta/R \ll 1$, the AB coupling is averaged out (fast-exchange limit) and the Hahn-echo decays with a rate on the order of Δ^2/R . The B -spin motion is so rapid that one might say that the A spins within the subset k , almost instantaneously after the first microwave ($\pi/2$) pulse, have traversed all frequencies invoked by the $A(i_k) B$ interac-

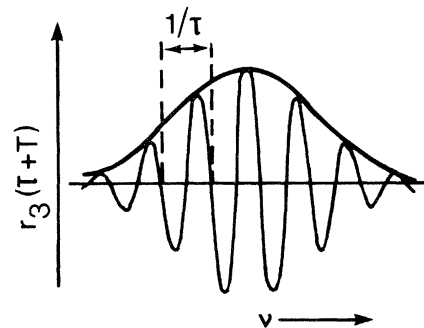


FIG. 1. Grating pattern as induced in an inhomogeneously broadened A -spin resonance line using a $\pi/2$ - τ - $\pi/2$ microwave pulse sequence.

TABLE I. Main spectroscopic properties of the (two-electron) F_2^{2+} center in MgO.

| Host | Absorption (nm) | No-phonon emission from triplet state (nm) | Fine- structure parameters (MHz) | Orientation magnetic axes | Polarization of radiation | Lifetime at 1.2 K |
|------|--------------------|--|---|---------------------------------|---------------------------------|-------------------------|
| MgO | 360 | 419 | $ D = 2555$ $ E = 236$ | $\hat{x} [001]$ | $\tau_x \ y$ | 12.5 ms |
| | | | | $\hat{y} [1\bar{1}0]$ | $\tau_y \ x$ | 27.5 ms |
| | | | | $\hat{z} [110]$ | τ_z | 1 s |

tion. As a result, long before the time τ (when the second pulse in the SE pulse cycle is applied), a stationary spectral distribution is reached. For our later discussion (cf. Sec. V), it is important to note that the mere existence of a stationary spectral distribution within the A -spin ensemble does not preclude the observation of a SE signal. The grating pattern imposed upon the inhomogeneously (strain-) broadened A -spin spectrum [as produced in the SE experiment by the application of two subsequent $\pi/2$ pulses separated in time by τ (see also Sec. III)] remains, even though the motional narrowing limit may apply for the AB -spin interactions. The B -spin fluctuations, when they give rise to the fast-exchange regime for the AB coupling, can never lead to a decay of the SE signal, however.

III. EXPERIMENTAL

A. Introduction

As already noted, in a stimulated-echo (SE) experiment a grating pattern is imposed upon an inhomogeneously broadened A -spin resonance line, and essentially one measures what is left of the grating after some time T (Ref. 10) (also see Fig. 1 and below). The grating pattern becomes (partly) erased due to nonstationary spectral diffusion and/or population decay out of the resonant A -spin levels. A convenient way to distinguish between the two possible contributions is to study the system by varying the periodicity of the grating. Certainly, one can not expect that when population decay determines the SED rate this rate will change when the grating periodicity is changed. On the other hand, when spectral diffusion is the determining factor for the SED rate, it is anticipated that the observed SED rate will depend on the periodicity of the frequency grating. The reason is that the diffusion kernel associated with the spectral-diffusion process exhibits a spectral dependence, i.e., the probability for a frequency jump of $\Delta\omega$ in frequency space depends on $\Delta\omega$ itself.

In MgO, the F_2^{2+} center consists of two electrons trapped at two neighboring oxygen anion vacancies, along a $[110]$ direction. The electronic structure of the defect is analogous to that of the H_2 molecule. Following optical absorption at 360 nm, a singlet state that is derived from the $1s2p$ configuration is excited. Subsequent (spontaneous) intersystem crossing populates the phosphorescent $^3B_{1u}$ level for which the intrinsic magnetic and optical properties have been studied in detail.^{11,12} Some of the principle spectroscopic properties of the F_2^{2+} centers in

MgO are summarized in Table I.

To outline the meaning of the various pulse steps in the spin-coherence experiments of this paper, the use of a Feynman-Vernon-Hellwarth (FVH) picture is convenient.^{2,3} In the FVH model a "pseudo" magnetization vector \vec{r} is introduced in an abstract space with orthogonal axes (e_1, e_2, e_3) so that

$$\vec{r} = (r_1, r_2, r_3) = ((\rho_{\beta\gamma} + \rho_{\gamma\beta}), i(\rho_{\beta\gamma} - \rho_{\gamma\beta}), (\rho_{\beta\beta} - \rho_{\gamma\gamma})),$$

where the latter denote elements of the density matrix ρ of the triplet spins in the basis $|\alpha\rangle, |\beta\rangle, |\gamma\rangle$. Coherence arises when the off-diagonal elements of ρ become nonzero ($\rho_{\beta\gamma}, \rho_{\gamma\beta} \neq 0$) or, equivalently, when r_1 or r_2 are nonzero. The behavior of \vec{r} is visualized geometrically from

$$\frac{d\vec{r}}{dt} = \vec{\Omega} \times \vec{r}, \quad (2)$$

where $\vec{\Omega}$ is specified by

$$\begin{aligned} \vec{\Omega} &= (\Omega_1, \Omega_2, \Omega_3) \\ &= ((V_{\beta\gamma} + V_{\gamma\beta}), i(V_{\beta\gamma} - V_{\gamma\beta}), (E_\beta - E_\gamma)), \end{aligned}$$

V being the time-dependent interaction between the triplet state and the microwave field of frequency ω pumping the $|\beta\rangle \rightarrow |\gamma\rangle$ transition. Noting the analogy between Eq. (2) and Bloch's equation of motion in magnetic resonance, one readily infers under what conditions the coherence component r_1 , which is equivalent to the S_1 magnetization mentioned earlier, is created. For the F_2^{2+} center in the phosphorescent $^3B_{1u}$ state, the so-called "probe"-pulse method was applied to obtain the desired SED behavior. In particular, the microwaves [of frequency $\omega = \omega_{\beta\gamma} = (E_\beta - E_\gamma)/\hbar$] were pulsed in the sequence given by $\pi/2 - \tau - \pi/2 - T - \pi/2 - \tau - \pi/2$. The meaning of this sequence follows from the FVH picture. The first $\pi/2$ pulse creates, for the F_2^{2+} triplet spins, a S_1^* magnetization which rapidly decays into a disk of phase-dispersed isochromats. At time τ (which is shorter than the characteristic phase memory time T_M), the second $\pi/2$ pulse causes a tilt of all isochromat moments over 90° . A net vertical magnetization results, the amplitude of which can be regarded as the superposition of weighted contributions of the individual isochromats. The weighting factor is determined by the time lag between the first two $\pi/2$ pulses and gives rise to a grating of the A -spin line, as illustrated in Fig. 1. The residual grating after a time interval T gives rise to a stimulated echo at the time $2\tau + T$

when a third $\pi/2$ pulse at $\tau+T$ is applied. Finally, the echo is probed optically by restoring the coherence component $S_1^*(2\tau+T)$ along the vertical axis in the FVH frame by means of the final $\pi/2$ pulse. In this way, the coherence is converted into an optically observable population difference between the resonant τ_z and τ_x ${}^3B_{1u}$ sublevels.

As will be discussed in Sec. V, our SED results as a function of τ prove unequivocally that spectral diffusion occurs in the nonstationary diffusion regime. It will be shown that the A spins, due to this diffusion, undergo relatively small frequency jumps (of the order of a few tens of kHz). This result is in agreement with the outcome of a number of additional spin-coherence experiments. In these experiments the system is studied from a somewhat different point of view, as indicated briefly now.

In an optically detected spin-locking experiment, a spin coherence $S_1^*(t)$ is formed which is locked to the microwave H_1 component by phase-shifting the H_1 field over 90° in the rotating frame.¹⁷⁻¹⁹ Of interest then is the decay with time of the field-locked spin coherence. The decay arises due to either a T_1 -type relaxation process or a spectral-diffusion process. In case of the latter, only frequency jumps larger than the precessional frequency associated with the locking field are effective. In a spin-ordering experiment the spins also become locked, but in a different fashion. Now, the spins are locked to their own local strain field in the crystal (by means of the technique of adiabatic demagnetization in the rotating frame^{6,20}). Decay of the spin-ordered state arises from T_1 relaxation or spectral diffusion, as in the spin-locking experiment, but now the diffusion process requires frequency jumps larger than the typical local-field values.

B. Samples and instrumental

Single crystals of additively colored MgO were the same as those used previously.^{11,12} The samples (cut from a single boule) contained a total anion-vacancy concentration of the order of $10^{18}/\text{cm}^3$. The crystal was mounted inside a slow-wave helix immersed in a He bath. Temperatures down to 1.2 K could be obtained by controlled pumping of the helium. For measurements in the range from 6 to 12 K, we used an Oxford Instruments He-flow cryostat. Light from a 100-W high-pressure mercury PEK lamp filtered by a water-cooled Schott UG-11 band pass filter was shone through the quartz windows in the cryostat onto the MgO crystal. The phosphorescence emitted perpendicular to the excitation pathway was focused on the entrance slit of a Monospek-1000 grating monochromator. For photodetection an RCA GaAs photomultiplier tube was used. The detection wavelength was chosen at the maximum of the phonon-side band of the F_2^{2+} -center emission at 435 nm.²¹

Microwaves generated in a HP 8690 B sweep oscillator unit outfitted with a (2-4)-GHz backward wave oscillator were amplified by a 20-W Varian Associates traveling-wave tube (VZC-6961). The microwaves were coupled by coaxial lines to a semirigid cable in the cryostat, which at its end supported the helix. Microwave-pulse trains were obtained by the appropriate switching of $p-i-n$ diodes in

the microwave circuit.

The pulse sequence for the $p-i-n$ diodes was delivered by a home-built pulse generator described in detail elsewhere.⁶ The generator also provided the reference pulse for the Princeton Applied Research lock-in amplifier. The lock-in-amplifier output was fed into a Varian Associate C-1024 CAT device for which the time base was synchronized with the scanned decay-time interval. The stimulated-echo-decay experiments were performed applying a $\pi/2-\tau-\pi/2-T-\pi/2-\tau-\pi/2$ pulse cycle at a repetition rate of approximately 10 Hz, the microwave frequency being set resonant with the $|D|-|E|$ transition at 2.319 GHz. Prior to the SED experiment, the $\pi/2$ -pulse duration was determined in a transient nutation experiment which monitors the phosphorescence-intensity changes as a function of the microwave-pulse length.¹⁹

In the SED experiment, changes in the F_2^{2+} -center emission associated with a variation of T were detected for a constant value of the parameter τ . Spin-locking was detected through the use of the probe-pulse method again. Now, the microwave-pulse sequence is $\pi/2-90^\circ-\tau_1-90^\circ-\pi/2$, where τ_1 denotes the lock time and a different notation is used for the pulse length ($\pi/2$) and phase shift (90°). Spin ordering was achieved by adiabatic demagnetization in the rotating frame, i.e., by an initial $(\pi/2, 0^\circ)$ pulse followed by a 90° phase-shifted locking which lasted about 100 μs , after which the microwave power was gradually reduced and the spin-ordered state was obtained. Detection of residual ordering after a time τ_0 was performed by applying a $(\pi/2, 0^\circ)-\tau-(\pi, 0^\circ)-\tau'-(\pi/2, 90^\circ)$ cycle which produces a derivativelike signal when τ' is scanned.⁶ Via measurement of the signal amplitude as a function of τ_0 , the characteristic decay time of the ordered signal was obtained. Finally, to measure the lifetimes of the individual ${}^3B_{1u}$ sublevels, we used the microwave-induced delayed-phosphorescence (MIDP) technique first introduced by Schmidt *et al.*²² The method allows one to determine the population decay rate of thermally isolated

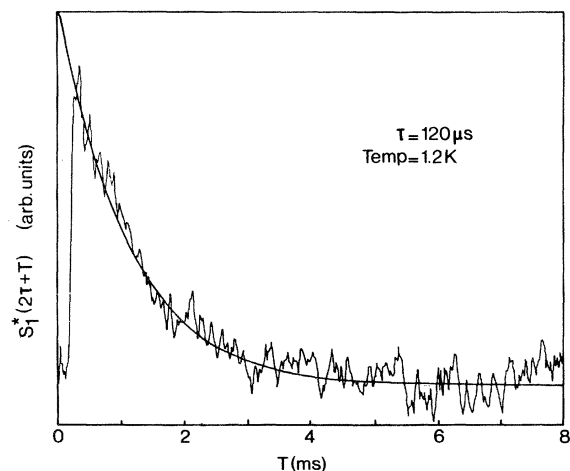


FIG. 2. Optically detected stimulated-echo decay as observed for the F_2^{2+} center in MgO in its photoexcited ${}^3B_{1u}$ state at 1.2 K using a $\pi/2-\tau-\pi/2-T-\pi/2-\tau-\pi/2$ pulse cycle (10 Hz) with $\nu=2.319$ GHz and $\tau=120$ μs . Drawn curve is monoexponential fit with a characteristic decay time of 1.15 ms.

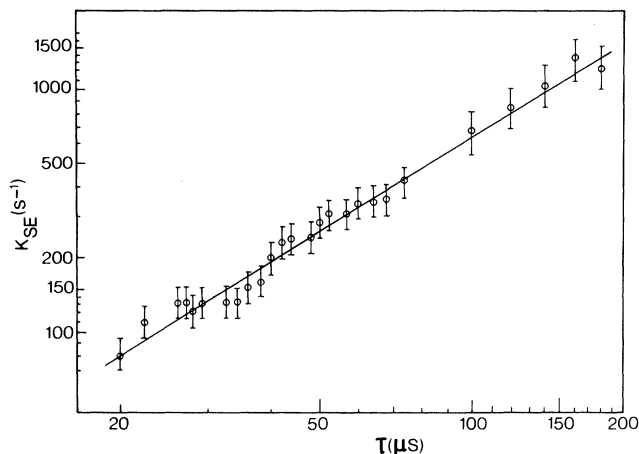


FIG. 3. Behavior of the characteristic decay rate of the stimulated-echo amplitude (after correcting for the population decay out of the τ_x and τ_z sublevels) as a function of the inverse grating period (τ) as obtained for the $|D\rangle - |E\rangle$ transition of the F_2^{2+} center in MgO in its photoexcited $^3B_{1u}$ state. Error bars are representative of the variation in k_{SE} as allowed for by the noise in the SED signal.

emissive and nonemissive substates. By mounting a chopper in the exciting-light pathway, the $^3B_{1u}$ state was populated by light pulses and allowed to decay completely in the dark period. During the dark period, a microwave pulse saturating one of the $^3B_{1u}$ -state spin transitions was applied, and the phosphorescence transients brought about by these pulses sampled by a Varian Associates CAT averaging device. The average output was fed into a HP 9825 B computer, and digitized for further analysis and data processing.

IV. RESULTS

A. Optically detected stimulated-spin-echo decays

Stimulated-spin-echo decays were obtained for the F_2^{2+} (MgO) centers in the $^3B_{1u}$ state. As an example, in

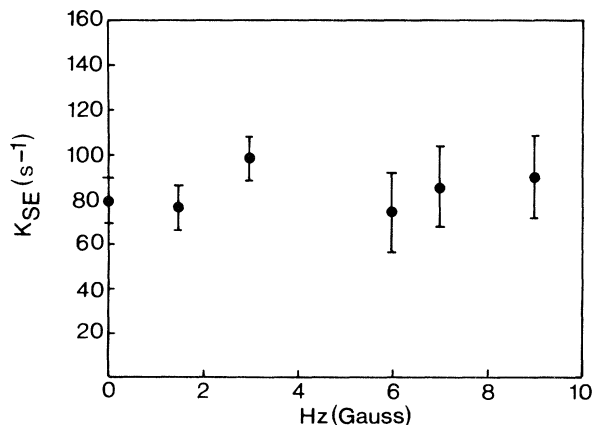


FIG. 4. Rate constants as obtained for the optically detected stimulated-spin-echo decay for the F_2^{2+} center in MgO at 2.319 GHz and 1.2 K as a function of the strength of a small externally applied magnetic field along the molecular z axis.

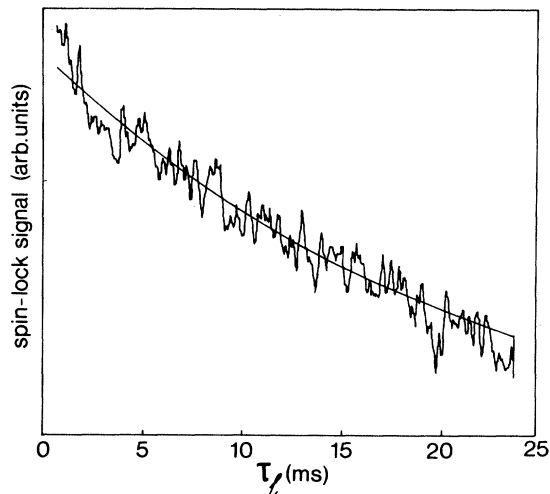


FIG. 5. Optically detected spin-locking decay at 2.319 GHz and 1.4 K for the F_2^{2+} center in MgO in zero field. Drawn line is monoexponential fit with $\tau_{\text{decay}} = 20$ ms.

Fig. 2 we present a SED obtained for the $\tau_z \leftrightarrow \tau_x$ zero-field transition at 2.319 GHz, for $\tau = 120 \mu\text{s}$. The drawn curve is the best fit; the experimental decay is monoexponential with a time constant of 1.15 ms. As discussed later, the decay of the stimulated-echo signal as a function of T is primarily due to nonstationary spectral diffusion. Support for this is obtained from another observation, namely the variation of the SED rate when the periodicity ($1/\tau$) in the grating of the inhomogeneously broadened optically detected magnetic resonance (ODMR) line is changed.

Figure 3 presents a log-log plot of the rate constant k_{SE} as a function of τ , where k_{SE} is the rate constant after correcting the SED for the population decay out of the τ_x and τ_z sublevels. Error bars are representative of the deviation in the decay rate constants allowed for by the noise in the measured decays. Reproducibility of the data and

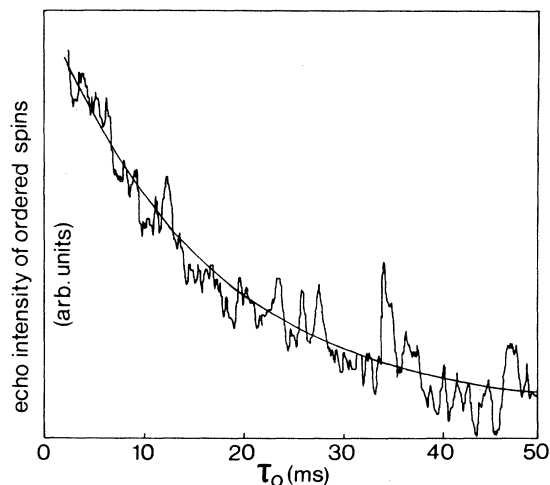


FIG. 6. Optically detected spin-echo decay in the ordered $^3B_{1u}$ state of the MgO F_2^{2+} center as monitored for the $|D\rangle - |E\rangle$ transition at zero field, $T = 1.4$ K. Drawn line is monoexponential fit with $\tau_{\text{decay}} = 16$ ms.

differences in the results among different samples (cut from the same boule) were well within the indicated error bars.

Previously, a drastic magnetic field effect on the Hahn-echo signals of the photoexcited F_2^{2+} center in MgO was reported.⁷ Similarly, experiments in the presence of an externally applied magnetic field were performed for the above-mentioned SED signals. Figure 4 presents the results for k_{SE} as a function of H_z as obtained in a series of SED experiments for which the grating period was kept constant. Clearly, no magnetic-field-induced effects on k_{SE} are found.

B. Spin locking and spin ordering

Representative decay signals for the spin-locked (SL) and spin-ordered (SO) states as observed for the $|D| - |E|$ transition within the $^3B_{1u}$ state of the F_2^{2+} center in MgO at 1.4 K are displayed in Figs. 5 and 6. The time constants deduced from the curves are (20 ± 4) ms for the SL decay and (16 ± 4) ms for the SO decay.

C. Microwave-induced delayed phosphorescence

Finally, results concerning the $^3B_{1u}$ -sublevel lifetimes are presented. Figure 7 shows the microwave-induced delayed phosphorescence (MIDP) response when, after the optical pulse, a series of microwave pulses resonant with the $|D| - |E|$ transition is applied at 1.2 K. From the MIDP signal two decay constants can be discerned. Of these, the fast component displays itself directly in the saturation recovery curves. These are characteristic of the radiative decay of the τ_x level for which a lifetime of (12.5 ± 1.0) ms was found. The slow component is obtained by plotting the discrete amplitudes $h(t)$ (cf. Fig. 7)

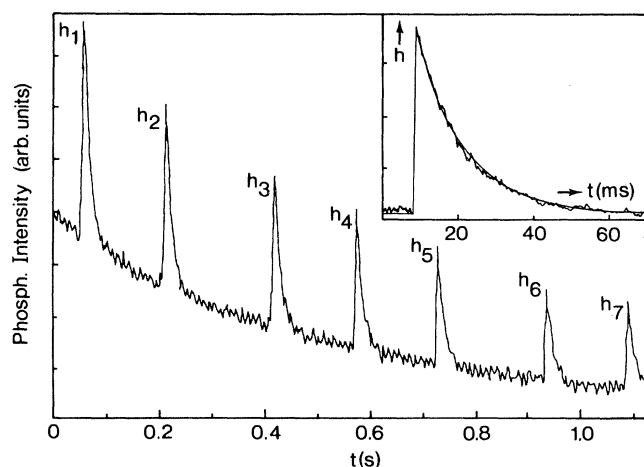


FIG. 7. Microwave-induced delayed-phosphorescence transients as induced by pulsing the $|D| - |E|$ transition at 2.319 GHz of the F_2^{2+} center in MgO, at a time t after the optical excitation pulse. The fast decay occurring after the (microwave) saturation pulse (the inset presents the fast decay on an enlarged scale) is representative of the radiative decay of the τ_x level. The lifetime of the τ_x level is determined as 12.5 ms. The slow decay as expressed by $h(t)$ is characteristic of the decay of the nonemissive τ_z level. The latter has a lifetime of 1 s.

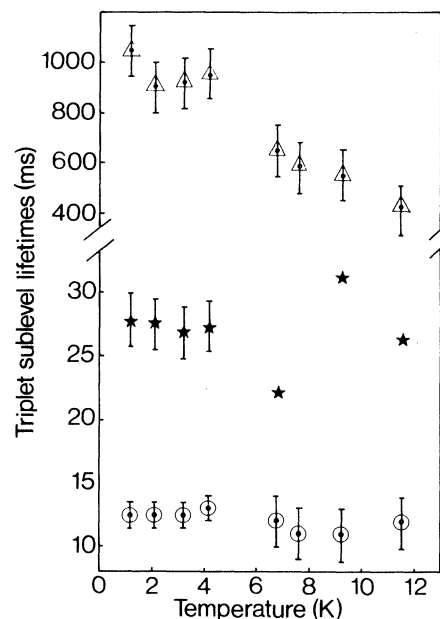


FIG. 8. Temperature dependence of the lifetimes of the $^3B_{1u}$ sublevels of the F_2^{2+} center in MgO as obtained from MIDP experiments. $\circ - \tau_x$, $* - \tau_y$, and $\triangle - \tau_z$.

versus t . The plot yields the characteristic decay time of the nonemissive τ_z level. This time was found as (1.00 ± 0.05) s.

The MIDP experiments were performed for temperatures ranging from 1.2 up to 12 K. The results are presented in Fig. 8. For $1.2 < T < 4.2$ K, the triplet-sublevel lifetimes were temperature independent. At higher temperatures, the lifetime of the τ_z substate showed a slight decrease. Apparently, spin-lattice relaxation comes into play for this level, although this additional relaxation still does not influence the τ_x - and τ_y -level lifetime. All in all, the MIDP experiments clearly show that, up to 12 K, the population decay of the $^3B_{1u}$ -state sublevels is slower than the SED of Fig. 2.

V. DISCUSSION

A. Three-pulse versus two-pulse echo decays

The fact that the characteristic stimulated-echo-decay times are shorter than the $^3B_{1u}$ -sublevel lifetimes (cf. Table I) rules out the possibility of population relaxation as a mechanism for the stimulated-echo decay. Evidently, the observed SED must be caused by spectral diffusion. This is also concluded from the τ dependence of k_{SE} (cf. Fig. 3). This effect demonstrates that more time is needed to smooth out a grating containing less undulations, as expected for diffusion in the frequency domain.

For F_2^{2+} centers in MgO in the photoexcited $^3B_{1u}$ state, spectral diffusion has previously also been concluded from optically detected Hahn-echo decays.⁷ From a study of the irreversible dephasing in the presence of an externally applied magnetic field, the dominant influence of spin-spin interactions among the probed F_2^{2+} -center spins and fluctuating nearby $I = \frac{5}{2}$ spins of the 10%

abundant ^{25}Mg isotope could be shown. To explore the possible connection between this dephasing mechanism and the observed SED's, we first recall an important feature of the Hahn-echo decays. The latter showed nuclear modulations when a small magnetic field ($H_z < 15$ G) was applied along the molecular z axis of the F_2^{2+} center. It has been argued that a prerequisite for the observation of the ^{25}Mg nuclear-spin-induced branching is that the AB -coupling strength is sufficiently large not to be averaged out by rapid B -spin flippings. Experimentally, the triplet- (A -) spin magnetic moment could be affected by changing the magnitude of H_z . In doing so, the AB coupling is influenced as well. Upon reduction of H_z to values below a few gauss, the nuclear modulations on the two-pulse echo decay had disappeared indicating that at zero field the fast- or intermediate-motion limit is attained. As discussed above in Sec. II, for the fast-motion limit one cannot observe nonstationary diffusion phenomena. It is evident therefore that the spectral diffusion probed in the SED experiments cannot be accounted for by the same dynamical interactions which give rise to irreversible dephasing of the triplet spins.

The same conclusion is arrived at from SED experiments in the presence of a magnetic field H_z . Previously, it was shown⁷ that a drastic decrease of the $^3B_{1u}$ -state phase memory time T_M is found when H_z is increased. The effect shows that dephasing is enhanced when a magnetic field is applied. The reason is, of course, the lifting of the A -spin magnetic-moment quenching, and hence an amplification of the AB -spin coupling. If the nonstationary A -spin diffusion, as observed from the SED's, would involve the same AB -spin-diffusion process, one would anticipate that an increase of H_z would also produce an enhanced SED rate. However, the results of Fig. 4 show that k_{SE} is independent of the magnetic field strength, and it is concluded again that, while the phase relaxation of the F_2^{2+} centers in the $^3B_{1u}$ state is governed by the magnetic dipole-dipole interaction with neighboring ^{25}Mg spins, the SED does not originate in these spin-spin interactions.

B. Spectral diffusion

Figure 3 reflects that when the grating period ($1/\tau$) in the SED experiment is increased, the rate for establishing the equilibrated pattern is decreased. The spreading out of the excitations in frequency space as time progresses is usually expressed by the diffusion kernel $K(\omega_f - \omega_i, t)$. This kernel is defined as the frequency distribution function after time t , given that the system initially has a frequency ω_i . As discussed by Mims,¹⁰ the SED function $D(\tau, T)$ is the Fourier transform of the diffusion kernel $K(\omega_f - \omega_i, T)$. Expressions for $D(\tau, T)$ are therefore readily obtained in the event of Gaussian or Lorentzian diffusion. Assuming, e.g., a Gaussian kernel with a mean-square linewidth proportional to the SE time T , one derives

$$D(\tau, T) \propto \exp(-2k\tau^3/3 - k\tau^2T);$$

analogously, for a Lorentzian diffusion with a linewidth proportional to T , one finds

$$D(\tau, T) \propto \exp(-m\tau^2 - m\tau T).$$

From an inspection of the log-log plot of Fig. 3, it is clear that the nonstationary diffusion probed in this work is predominantly of Lorentzian nature. The slope of 1.28 is indicative of a slight deviation towards a more Gaussian-shaped function. A Lorentzian kernel is expected when a A -spin environment is nonuniform, and, due to this, some A spins on the average experience larger frequency fluctuations than others, thus giving rise to more pronounced wings of the diffusion kernel than in the ordinary Gaussian shape. For a small fraction of the A spins, the frequency jumps may be so large that within the time τ they have dephased, and thus escape observation in the stimulated-echo experiment. The latter effect will tend to increase the Gaussian character of the diffusion, and thus may be responsible for the slight deviation of the slope in Fig. 3 from the value 1. At any rate, the predominantly Lorentzian diffusion is evidence that the F_2^{2+} centers experience nonuniform time-dependent environments which, as was seen earlier, cannot be caused by B -spin fluctuations.

As noted above, a substantial averaging out of the hyperfine coupling between the $S=1$ F_2^{2+} -center spins and the $I = \frac{5}{2}$ ^{25}Mg spins takes place at zero field, $T=1.2$ K. Under these circumstances it is meaningful to consider the phase memory time T_M (obtained from the two-pulse echo decays) as representative of the inverse of the homogeneous linewidth. When we now compare the homogeneous width obtained from the two-pulse echo decay, i.e., $\Delta\nu = 1/(\pi T_2) \simeq 2$ kHz, with applied grating periods in the SE experiments, i.e., values between 10 kHz and 1 MHz, we readily see that the SE experiments yield information regarding the filling in of holes wider than the homogeneous width but still only within the kHz range. The evolution of the diffusion kernel with time according to a Lorentzian shape shows that small frequency steps are more probable than large steps. This is the reason that the time needed to diffuse over an interval as large as 1 MHz (i.e., $\tau = 1 \mu\text{s}$) is long compared to the time constant for decay out of the $^3B_{1u}$ state to the ground state (cf. Table I). This result is in agreement with the findings from spin-locking (SL) and spin-ordering (SO) decay experiments.

From a comparison of the SL and SO decay times with the sublevel lifetimes given in Table I, it follows that the SL and SO decays are almost completely due to the process of radiative decay of the τ_x level to the ground state. By taking into account that the microwave H_1 field used for spin locking is approximately 3 MHz (as determined from a transient nutation experiment) and that the spin-locked signal is sensitive to frequency jumps only larger than γH_1 , it follows from the SL experiment that spin fluctuations within the A -spin ensemble do not surpass 3 MHz. Analogously, the SO experiment shows that spins ordered in either the τ_z or τ_x level by their local field, do not diffuse sufficiently far to disrupt the ordering in a noticeable fashion during the triplet lifetime. Apparently,

the diffusion in the kHz frequency range as detected by the SED's is not resolved in the SL and SO decays, and the application of the SE technique is essential for exposing the small-step spin diffusion of the F_2^{2+} centers in MgO.

C. Energy transfer or electron tunneling

Let us now turn to the mechanism for the nonstationary spectral diffusion of the three-pulse echo experiments. It was already noted that diffusion due to B -spin fluctuations can be excluded. An alternative is to consider diffusion through the inhomogeneous F_2^{2+} -center ODMR line on account of a transfer of the optical excitation among distinct F_2^{2+} -center sites in the host crystal. The concentration of oxygen-vacancy centers, in the additively colored MgO crystals, is estimated to be 10^{18} cm^{-3} .¹² On the average, the separation between the defects is then approximately 10^2 \AA , which distance hardly seems to favor effective energy transfer, even on the basis of dipole-dipole interactions.²³ On the other hand, if some defect clustering in the crystal occurs, energy transfer is readily conceivable. In additively colored CaO, the grouping of defect centers has recently been shown to be sufficiently close for electron tunneling to take place between F_A^+ and photoexcited F centers.²⁴ Similar processes have been suggested in additively colored MgO.²⁵ We propose that the spectral diffusion observed here in the microwave region is produced by either the transfer of optical energy among F_2^{2+} centers or electron tunneling involving F -type defects. The predominantly Lorentzian character of the diffusion process (see the discussion above) is further support that randomly distributed F_2^{2+} centers are involved.

We found no temperature effects on the SE-decay rates below 4.2 K. Evidently, a resonant transfer process is implied in the microwave region. This finding is compatible with our earlier notion that the diffusion proceeds by a random walk of small steps in frequency space. Of course, more work is needed to further substantiate the proposed mechanism of excitation (electron) transfer as the cause for the observed spectral diffusion. Experiments along these lines, using laser-selective excitation, is in progress in this laboratory.

VI. CONCLUSION

The stimulated-echo-decay results presented in this work clearly show that photoexcited F_2^{2+} centers in MgO

exhibit the phenomenon of nonstationary spectral diffusion through the inhomogeneously broadened $|D| - |E|$ transition within the $^3B_{1u}$ state. The mechanism underlying the spectral-diffusion process cannot be the same as that which is applicable for the irreversible dephasing among the triplet spins for a simple reason. Earlier work on the same system had shown⁷ that magnetic dipole-dipole couplings to other (fluctuating) spins in the lattice is almost averaged out in zero field mainly because of the weak $S=1$ magnetic moment. Here, spectral averaging means that the spin dipole-dipole interactions do not contribute to the inhomogeneous broadening of the triplet- (A -) spin resonances, and hence it would be inconsistent to suggest at the same time that B -spin flippings induce diffusion through such an inhomogeneous contribution to the spectrum. This conclusion could be confirmed experimentally in the presence of an applied magnetic field: whereas the Hahn-echo decays are extremely sensitive to small fields, no field effects could be detected on the SED's. Thus it appears that the F_2^{2+} -center spin system presents a clear example of a situation that two-pulse and three-pulse echo measurements on the same system expose different kinds of spectral-diffusion processes.

Now that spin-spin couplings can be excluded in considering the inhomogeneous broadening of the $^3B_{1u}$ -state spin transitions, this broadening must be due solely to crystal imperfections such as random strain fields, electric fields, etc. The observation of spin diffusion then necessarily must imply random time-dependent changes of these local fields. In Sec. V we proposed a random migration of the optical excitation energy of the $^3B_{1u}$ state through the lattice, or, alternatively, an electron tunneling process involving randomly distributed oxygen-vacancy centers. As expected for diffusing spins experiencing nonuniform surroundings, a predominantly Lorentzian diffusion could be concluded from the behavior of k_{SE} as a function of the grating period ($1/\tau$). Finally, no temperature effects up to 4.2 K were found for k_{SE} . This finding excludes the assistance of phonons in the excitation (or electron) transfer process at liquid-helium temperatures.

ACKNOWLEDGMENTS

This work was supported in part by the Netherlands Foundation for Chemical Research (SON) with financial aid from the Netherlands Organization for the Advancement of Pure Research (Nederlandse Organisatie voor Zuiver-Wetenschappelijk Onderzoek).

¹For a recent review, see M. J. Burns, W. K. Liu, and A. H. Zewail, in *Spectroscopy and Excitation Dynamics of Condensed Molecular Systems*, edited by V. Agranovich and R. Hochstrasser (North-Holland, Amsterdam, 1983), p. 301.

²C. B. Harris and W. G. Breiland, in *Laser and Coherence Spectroscopy*, edited by J. I. Steinfeld (Plenum, New York, 1978), p. 373.

³J. Schmidt and J. H. van der Waals, in *Time Domain Electron*

Spin Resonance, edited by L. Kevan and R. N. Schwartz (Wiley, New York, 1979), p. 343.

⁴H. C. Brenner, in *Triplet State ODMR Spectroscopy*, edited by R. H. Clarke (Wiley, New York, 1982), p. 185.

⁵D. J. Gravesteijn, J. H. Scheijde, and M. Glasbeek, *Phys. Rev. Lett.* **39**, 105 (1977).

⁶M. Glasbeek and R. Hond, *Phys. Rev. B* **23**, 4220 (1981); R. Hond, and M. Glasbeek, *Phys. Rev. B* **26**, 427 (1982).

- ⁷M. W. L. Bovy and M. Glasbeek, *J. Chem. Phys.* **76**, 1676 (1982).
- ⁸A. Szabo, *Phys. Rev. Lett.* **25**, 924 (1970).
- ⁹P. N. Prasad, J. R. Morgan, and M. A. El-Sayed, *J. Phys. Chem.* **85**, 3569 (1981).
- ¹⁰W. B. Mims, in *Electron Paramagnetic Resonance*, edited by S. Geschwind (Plenum, New York, 1972), p. 263.
- ¹¹M. Glasbeek, R. Sitters, and B. Henderson, *J. Phys. C* **13**, L1012 (1980).
- ¹²B. Henderson, M. Yamaga, M. Glasbeek, and R. Sitters, *J. Phys. C* **14**, 2505 (1981).
- ¹³B. J. Berne, in *Statistical Mechanics, Part B: Time-Dependent Processes*, edited by B. J. Berne (Plenum, New York, 1977), p. 233.
- ¹⁴A. R. Burns, M. A. El-Sayed, and J. C. Brock, *Chem. Phys. Lett.* **75**, 31 (1980).
- ¹⁵J. R. Klauder and P. W. Anderson, *Phys. Rev.* **125**, 912 (1962).
- ¹⁶W. B. Mims, *Phys. Rev.* **168**, 370 (1968).
- ¹⁷C. P. Slichter and W. C. Holton, *Phys. Rev.* **122**, 1701 (1961).
- ¹⁸C. B. Harris, R. L. Schlupp, and H. Schuch, *Phys. Rev. Lett.* **30**, 1019 (1973).
- ¹⁹D. J. Gravesteijn and M. Glasbeek, *Phys. Rev. B* **19**, 5549 (1979).
- ²⁰H. C. Brenner, J. C. Brock, and C. B. Harris, *J. Chem. Phys.* **60**, 4448 (1974).
- ²¹J. D. Bolton, B. Henderson, and D. O. O'Connell, *Solid State Commun.* **38**, 287 (1981).
- ²²J. Schmidt, D. A. Antheunis, and J. H. van der Waals, *Mol. Phys.* **22**, 1 (1971).
- ²³R. Orbach, in *Optical Properties of Ions in Solids*, edited by B. di Bartolo (Plenum, New York, 1975), p. 355.
- ²⁴F. J. Ahlers, F. Lohse, and J. M. Spaeth, *Solid State Commun.* **43**, 321 (1982).
- ²⁵G. P. Summers, T. M. Wilson, B. T. Jeffries, H. T. Tohver, Y. Chen, and M. M. Abraham, *Phys. Rev. B* **27**, 1283 (1983).